Optimization of WAVE2 complex–induced actin polymerization by membrane-bound IRSp53, PIP_3, and Rac

Shiro Suetsugu,[1,2] Shusaku Kurisu,[1,2] Tsukasa Oikawa,[1,2] Daisuke Yamazaki,[1,2] Atsushi Oda,[3] and Tadaomi Takenawa[1,2]

[1]Department of Biochemistry, Institute of Medical Science, University of Tokyo, Minato-ku, Tokyo 108-8639, Japan
[2]Core Research for Evolutional Science and Technology, Japan Science and Technology Corporation, Kawaguchi 332-0012, Japan
[3]Laboratory of Environmental Biology, Department of Preventive Medicine, Hokkaido University School of Medicine, Kitaku, Sapporo 060-8638, Japan

WAVE2 activates the actin-related protein (Arp) 2/3 complex for Rac-induced actin polymerization during lamellipodium formation and exists as a large WAVE2 protein complex with Sra1/PIR121, Nap1, Abi1, and HSPC300. IRSp53 binds to both Rac and Cdc42 and is proposed to link Rac to WAVE2. We found that the knockdown of IRSp53 by RNA interference decreased lamellipodium formation without a decrease in the amount of WAVE2 complex. Localization of WAVE2 at the cell periphery was retained in IRSp53 knockdown cells. Moreover, activated Cdc42 but not Rac weakened the association between WAVE2 and IRSp53. When we measured Arp2/3 activation in vitro, the WAVE2 complex isolated from the membrane fraction of cells was fully active in an IRSp53-dependent manner but WAVE2 isolated from the cytosol was not. Purified WAVE2 and purified WAVE2 complex were activated by IRSp53 in a Rac-dependent manner with PIP_3-containing liposomes. Therefore, IRSp53 optimizes the activity of the WAVE2 complex in the presence of activated Rac and PIP_3.

Introduction

Activation of phosphatidylinositol (PI)-3-kinase and small GTPases at the cell membrane controls various intracellular events, including cell–cell junction formation (Bershadsky, 2004), extension of the leading edge (Ridley et al., 2003), and infectious processes of pathogens (Cossart and Sansonetti, 2004). Activation of PI-3-OH kinase and subsequent PIP_3 production activates Rac through PIP_3 binding to Rac guanine nucleotide exchange factors (Rickert et al., 2000; Chung et al., 2001). PIP_3 is a lipid component of the cell membrane, and Rac is integrated into the membrane via lipid modification (Hall, 1998). Therefore, the site of action downstream of PIP_3 and Rac should be the membrane.

WAVE2 belongs to the Wiskott-Aldrich syndrome protein (WASP) family of proteins, which activate the actin-related protein (Arp) 2/3 complex to stimulate signal-induced actin polymerization. Five WASP family proteins have been identified, and WAVE1, WAVE2, and neural WASP (N-WASP) are expressed ubiquitously (Suetsugu et al., 1999; Takenawa and Miki, 2001). Studies of cells from WAVE1, WAVE2, and N-WASP knockout mice have shown that WAVE2 is the protein that activates the Arp2/3 complex downstream of the small GTPase Rac (Snapper et al., 2001; Suetsugu and Takenawa, 2003; Yan et al., 2003). We have reported that WAVE2 is a PIP_3-binding protein, although PIP_3 alone was not involved in regulating the ability of WAVE2 to activate the Arp2/3 complex (Oikawa et al., 2004).

A large protein complex has been proposed to suppress WAVE1 activity by trans-inhibition in which a trimeric protein complex, including PIR121/Sra1, Nap1, and Abi, binds to WAVE1 and suppresses WAVE1 activity (Eden et al., 2002). WAVE2 also forms a large protein complex including HSPC300, Abi1, Nap1, and Sra1/PIR121 (Kunda et al., 2003; Rogers et al., 2003; Gautreau et al., 2004; Innocenti et al., 2004; Steffen et al., 2004). Studies of cultured cells have shown that Sra1, Nap1, and Abi are involved in stabilizing WAVE2; the knockdown of Abi1, Nap1, or Sra1 results in decreased amounts of all of the proteins in the WAVE2 complex (Kunda et al., 2003; Rogers et al., 2003; Steffen et al., 2004). Among proteins in the WAVE2 complex, Abi1 and HSPC300 bind directly to the NH_2-terminal

Correspondence to Tadaomi Takenawa: takenawa@ims.u-tokyo.ac.jp

Abbreviations used in this paper: Arp, actin-related protein; CA, constitutively active; DN, dominant negative; IMD, IRSp53/missing in metastasis homology domain; IRTKS, insulin receptor tyrosine kinase substrate; MEF, mouse embryonic fibroblast; PC, phosphatidylcholine; PI, phosphatidylinositol; SH3, Src homology 3; N-WASP, neural WASP; RCB, Rac binding; WASP, Wiskott-Aldrich syndrome protein; WHD, WAVE homology domain.

The online version of this article contains supplemental material.

The Journal of Cell Biology, Vol. 173, No. 4, May 22, 2006 571–585
http://www.jcb.org/cgi/doi/10.1083/jcb.200509067

WAVE homology domain (WHD) of WAVE2. WHD-mediated association with Abi1/2 also contributes to the localization of WAVE2 at the leading edge of lamellipodia (Leng et al., 2005). However, purified HSPC300, Abi1, Nap1, and Sra1/PIR121 do not suppress the activity of WAVE2 purified from a baculovirus system (Gautreau et al., 2004; Innocenti et al., 2004). Therefore, trans-inhibition does not appear to occur with WAVE2 purified from baculovirus. The activity of the native WAVE2 complex has yet to be examined.

A WAVE2-binding protein that is not included in the aforementioned protein complex is IRSp53/BAIAP2/Bap2α (Miki et al., 2000). The Src homology 3 (SH3) domain of IRSp53 binds to WAVE2, and the NH_2-terminal Rac-binding (RCB) domain (residues 1–228) binds to Rac (Miki et al., 2000; Choi et al., 2005). Thus, IRSp53 might be the link between Rac and WAVE2 that is involved in lamellipodium formation. The NH_2-terminal region of IRSp53 (residues 1–250), including the RCB domain, is termed the IRSp53/missing in metastasis homology domain (IMD). The IMD possesses actin filament bundling activity, and the overexpression of IRSp53 induces microspike/filopodium formation (Govind et al., 2001; Krugmann et al., 2001; Millard et al., 2005). Furthermore, Cdc42 does not bind to the RCB domain but binds to the Cdc42–Rac interactive binding motif between the RCB and SH3 domains (Govind et al., 2001; Krugmann et al., 2001). These findings have not been reconciled, and the role of IRSp53 in actin cytoskeletal reorganization remains to be clarified.

In this study, we investigated the activity of the WAVE2 complex purified from various cellular preparations and examined the contributions of WAVE2-binding proteins to the regulation of WAVE2 downstream of Rac.

Results

Localization of WAVE2 and IRSp53

To purify the WAVE2 complex from cultured cells, we stably expressed WAVE2 tagged with FLAG in A431 cells. The amount of WAVE2 in the FLAG-WAVE2–expressing cell line was approximately twice that of control vector–transfected cells (Fig. S1 A, available at http://www.jcb.org/cgi/content/full/jcb.200509067/DC1). This cell line and the control cell line were used throughout this study. WAVE2 in FLAG-WAVE2–expressing cells was localized similar to WAVE2 in control A431 cells (Fig. S1 A). A significant portion of endogenous WAVE2 localized at cell–cell junctions and lamellipodia (Fig. 1 A).

In cells with decreased Abi1 expression by RNAi, the amount of WAVE2 was significantly decreased in FLAG-WAVE2–expressing cells, indicating that tagged WAVE2 under stable expression behaved similarly to endogenous WAVE2 (Fig. 1 C). WAVE2 tagged with GFP did not localize properly in the absence of Abi1, but it localized in a manner similar to endogenous WAVE2 in the presence of Abi1 as reported previously, indicating that Abi1 is essential for the localization of WAVE2 (Fig. 1 B; Steffen et al., 2004; Leng et al., 2005).

We previously identified IRSp53 as a WAVE2-binding protein. The presence of IRSp53 splice variants was indicated by the presence of IRSp53 bands at two positions on the Western blot. IRSp53 was also localized at cell–cell junctions and lamellipodia (Fig. 1 A). In cells with decreased IRSp53 expression, the amount of WAVE2, Abi1, Nap1, or Sra1 in whole cell lysates was not altered (Fig. 1 C), and WAVE2 remained at the cell periphery (Fig. 1 A). The amount of Abi in the WAVE2 protein complex was not significantly altered by IRSp53 knockdown (Fig. S1 B), as indicated by immunoprecipitation with anti-FLAG antibody.

IRSp53 participates in lamellipodia formation

In cells subjected to IRSp53 RNAi, lamellipodium formation in response to EGF treatment or expression of constitutively active (CA) Rac (Rac CA) was significantly decreased (Figs. 1 A and 2, A and B). Time-lapse analysis confirmed the decrease in lamellipodium formation, especially the speed of extension at the leading edge of cells treated with IRSp53 RNAi (Fig. 1 D and Video 1, available at http://www.jcb.org/cgi/content/full/jcb.200509067/DC1). The reduction in speed of the extension of cells treated with Abi1 RNAi was more drastic than of cells treated with IRSp53 RNAi (Fig. 1 D and Video 1).

A similar protein, insulin receptor tyrosine kinase substrate (IRTKS), was also found in A431 cells by RT-PCR analysis (Fig. S1 B). RNAi for IRTKS was performed in A431 cells, and specific decreases in mRNA were observed for IRTKS (Fig. S1 B). However, the reduction of IRTKS did not affect ruffle formation (Fig. 1 A).

We then examined whether IRSp53 is essential for ruffle formation in fibroblasts. Mouse embryonic fibroblasts (MEFs) from WAVE2 knockout mice were used. The expression of full-length (wild type) WAVE2 restored ruffle formation upon the expression of Rac CA, but the expression of ΔPR WAVE2 with a deleted proline-rich region (IRSp53-binding region) or of ΔWHD WAVE2 with a deleted WHD region (Abi1-binding region) did not (Fig. S2, available at http://www.jcb.org/cgi/content/full/jcb.200509067/DC1). The A5 mutant of WAVE2 (defective in binding to PIP_3; Oikawa et al., 2004) also failed to restore ruffle formation (Fig. S2). Importantly, ΔPR WAVE2 localized at the cell periphery, whereas ΔWHD WAVE2 did not. Consistent with the localization of WAVE2 at the cell periphery in IRSp53 RNAi A431 cells (Fig. 1 A), IRSp53 was not essential for the localization of WAVE2. In MEFs, ruffle formation was severely impaired by Abi1 RNAi (Fig. S2 and Video 2). IRSp53 RNAi caused a decrease of ruffle formation and extension speed of the leading edge, indicating the involvement of IRSp53 in ruffle formation in fibroblasts (Fig. S2 and Video 2).

Negative regulation of WAVE2–IRSp53 association by Cdc42

Because IRSp53 binds to both Rac and Cdc42, we examined the interaction between IRSp53 and WAVE2 upon the expression of CA mutants. In the presence of Cdc42 CA, the interaction was significantly decreased (Fig. 2, C and D). In contrast, the interaction between IRSp53 and WAVE2 was not significantly perturbed by Rac CA expression (Fig. 2, C and D). The interaction between purified WAVE2 and purified IRSp53 was also decreased in the presence of GTPγS-loaded Cdc42 but not in the

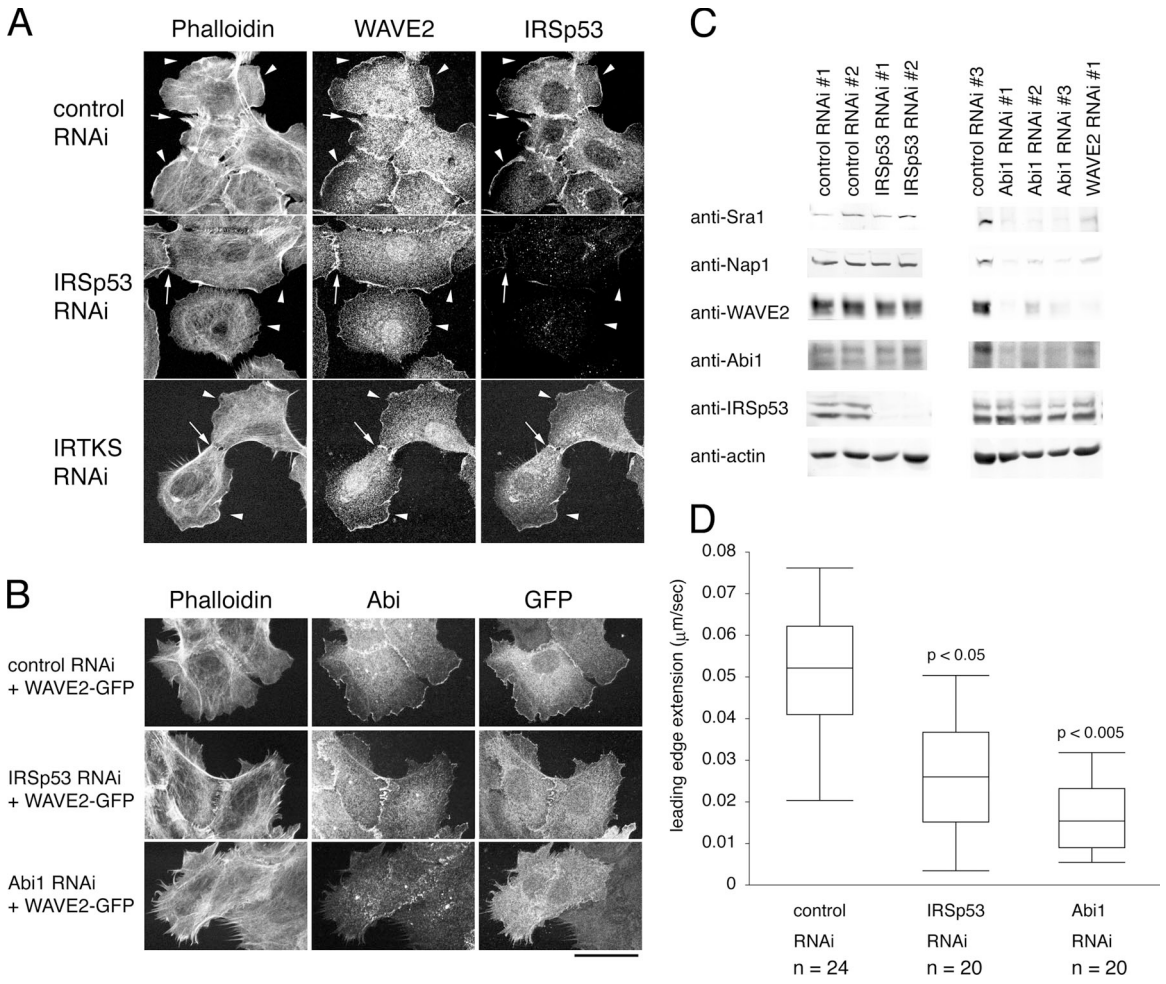

Figure 1. **Localization of WAVE2 and IRSp53 in A431 cells.** (A) Localization of WAVE2 and IRSp53 in EGF-stimulated A431 cells treated with control, IRSp53, or IRTKS stealth RNAi was examined by immunofluorescence with anti-WAVE2 antibody or anti-IRSp53 antibody (M051-3). Actin filaments stained with phalloidin are also shown. WAVE2 and IRSp53 were localized at ruffles (arrowheads) and cell–cell junctions (arrows). (B) Localization of WAVE2-GFP in A431 cells with reduced IRSp53 or Abi1 expression. A431 cells were transfected with WAVE2-GFP expression vector and pSuper vectors for control, IRSp53, or Abi1 RNAi. GFP signal was enhanced by anti-GFP staining. Bar, 40 μm. (C) Western blot analysis of whole cell lysates from control, IRSp53, or Abi1 stealth RNAi-treated A431 cells. Western blot with anti-actin antibody is shown as a loading control. (D) Quantification of the speed of the leading edge extension of EGF-stimulated A431 cells. Significant difference was analyzed by the *t* test. Error bars represent SD.

presence of Rac (Fig. 2 E). Therefore, Cdc42 appears to negatively regulate the binding of IRSp53 to WAVE2.

Enrichment of IRSp53 at the membrane and translocation of some WAVE2 to the membrane upon stimulation

We fractionated cells and examined the subcellular localization of proteins by conventional ultracentrifugation (Fig. 3 A). All of the proteins analyzed were found in all cell fractions, including the cytosol, membrane, and nucleus (unpublished data). WAVE2 was somewhat enriched in the membrane fraction; the membrane fraction contained 30% more WAVE2 than the cytosol fraction. Abi1 was much more enriched in the membrane fraction, as the membrane fraction contained approximately twice that of the cytosol fraction. Most IRSp53 was present in the membrane fraction, as it contained four times that of the cytosol fraction (Fig. 3 A).

We then examined whether ruffle-inducing stimuli could translocate WAVE2 from the cytosol and nucleus to the membrane. Upon EGF treatment, the amount of WAVE2 in the membrane fraction was increased 17% (Fig. 3, C and D). When Rac CA was expressed, the amount of WAVE2 in the membrane fraction increased 26% (Fig. 3 B). However, when dominant-negative (DN) Rac (Rac DN) was expressed, the amount of WAVE2 in the membrane fraction decreased 16% (Fig. 3, B and D). The expression of Cdc42 CA also decreased the membrane localization of WAVE2 (Fig. 3 D and S1 E). WAVE2 in the cytosol fraction was not significantly reduced in response to these stimuli, presumably because of the presence of nuclear WAVE2 translocated to the cytosol, as shown by antibody staining of the cells (unpublished data). Thus, ruffle-inducing stimuli induced the translocation of some WAVE2 to the membrane (Fig. 3 E). We then examined the contribution of IRSp53 to the membrane localization of WAVE2. When we knocked down IRSp53 by RNAi, the amount of WAVE2 at the membrane decreased by 30–40% (Fig. 3, B and D). WAVE2 was not involved in the membrane localization of IRSp53 because RNAi of WAVE2 did not have an effect on the amount of IRSp53 in the membrane (Fig. 3 E).

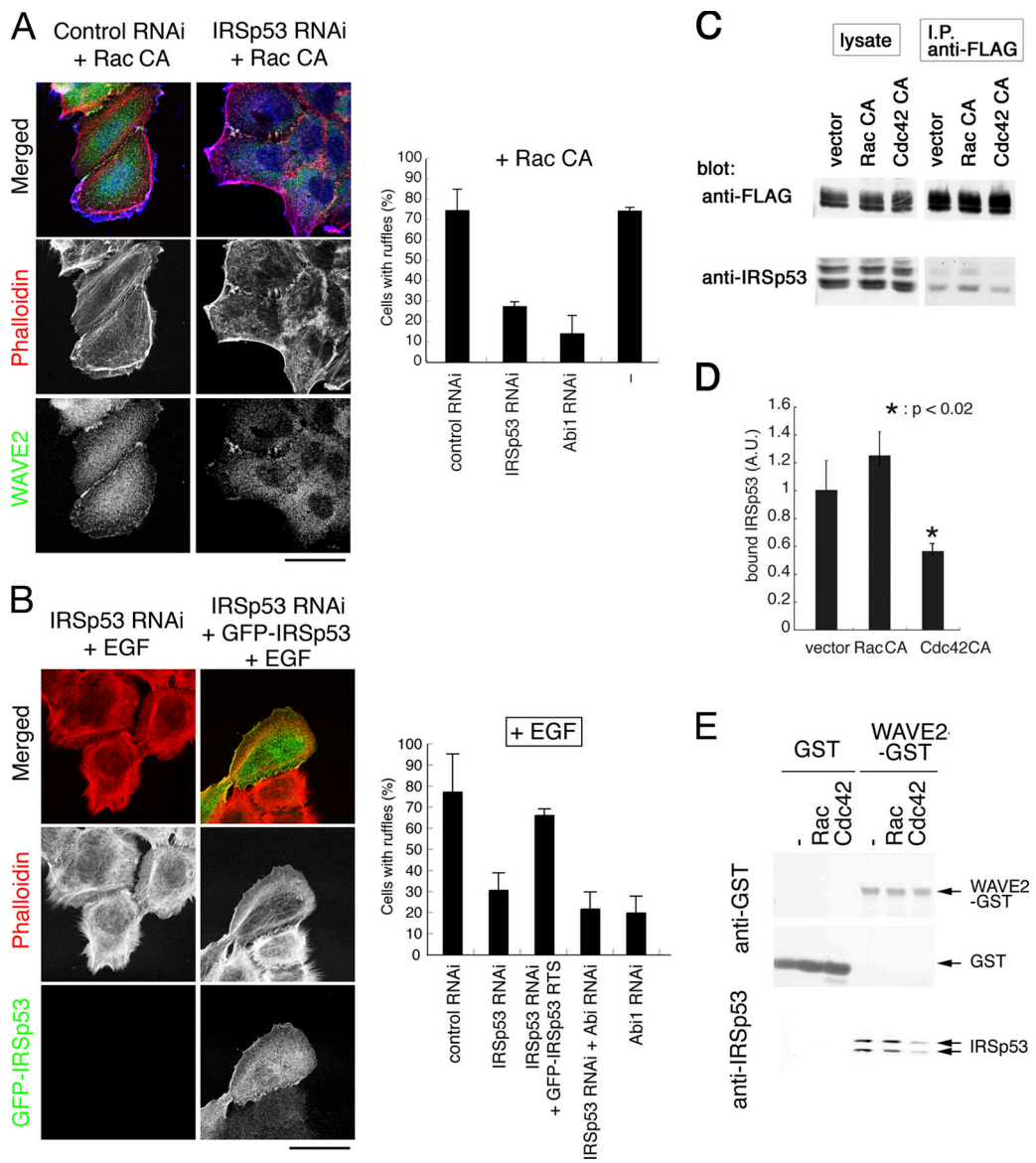

Figure 2. **Involvement of IRSp53 in Rac and EGF-induced ruffle formation in A431 cells.** (A) A431 cells were transfected with constitutively active Rac (Rac CA) and control or IRSp53 RNAi pSuper vector. (left) Actin filament (red; phalloidin) and WAVE2 localization (green; anti-WAVE2) was then analyzed. Rac expression is shown in blue. (right) Quantification of membrane ruffles in transfected cells. Three independent experiments were performed. (B) EGF-stimulated A431 cells transfected with IRSp53 RNAi pSuper vector alone or plus RNAi-resistant GFP-IRSp53 expression vector. (left) Actin filament (red; phalloidin) and GFP localization (green; anti-GFP) were then analyzed. (A and B) Bars, 40 μm. (right) Quantification of membrane ruffles as in A. (C and D) A431 cells stably expressing FLAG-tagged WAVE2 were transfected with Rac CA or Cdc42 CA expression vector. Then, IRSp53 in the FLAG-WAVE2 precipitates was examined by Western blot analysis (C). The amount of IRSp53 relative to WAVE2 in the precipitate was quantified by densitometry (D). Three independent experiments were performed. (E) GST fusion protein of WAVE2 was immobilized, and purified IRSp53 was incubated with GTPγS-loaded Rac or Cdc42. After washing, bound IRSp53 was examined by Western blotting. Error bars represent SD.

Characterization of the WAVE2 complex from the membrane and cytosol fractions

To determine the relationship between protein localization and Arp2/3 complex activation, we purified WAVE2 protein complex with a FLAG tag. We purified WAVE2 complex from the cytosolic fraction; however, we were unable to resolubilize the pelleted membrane fraction. Therefore, we purified the WAVE2 complex from cell lysates, including the membrane fraction, with Triton X-100. Thus, WAVE2 complex from the Triton X-100 fraction contained cytosolic and membrane WAVE2 at a ratio of ∼1:1.3 (Fig. 3 A).

Examination of the proteins in the WAVE2 complex in the Triton X-100 fraction by Western blotting showed the presence of Abi1 and IRSp53, as reported previously (Fig. 4 A; Miki et al., 2000; Innocenti et al., 2004; Steffen et al., 2004). Abi1 also exists as several isoforms and splice variants, and several bands were identified. EGF stimulation induces the phosphorylation of WAVE2 (Miki et al., 1999). However, significant alterations in the amounts of Abi1 and IRSp53 in WAVE2 immunoprecipitates were not observed in response to EGF stimulation. Specific binding of IRSp53 and Abi to WAVE2 was confirmed in experiments with vector-transfected cells (Fig. 4 A).

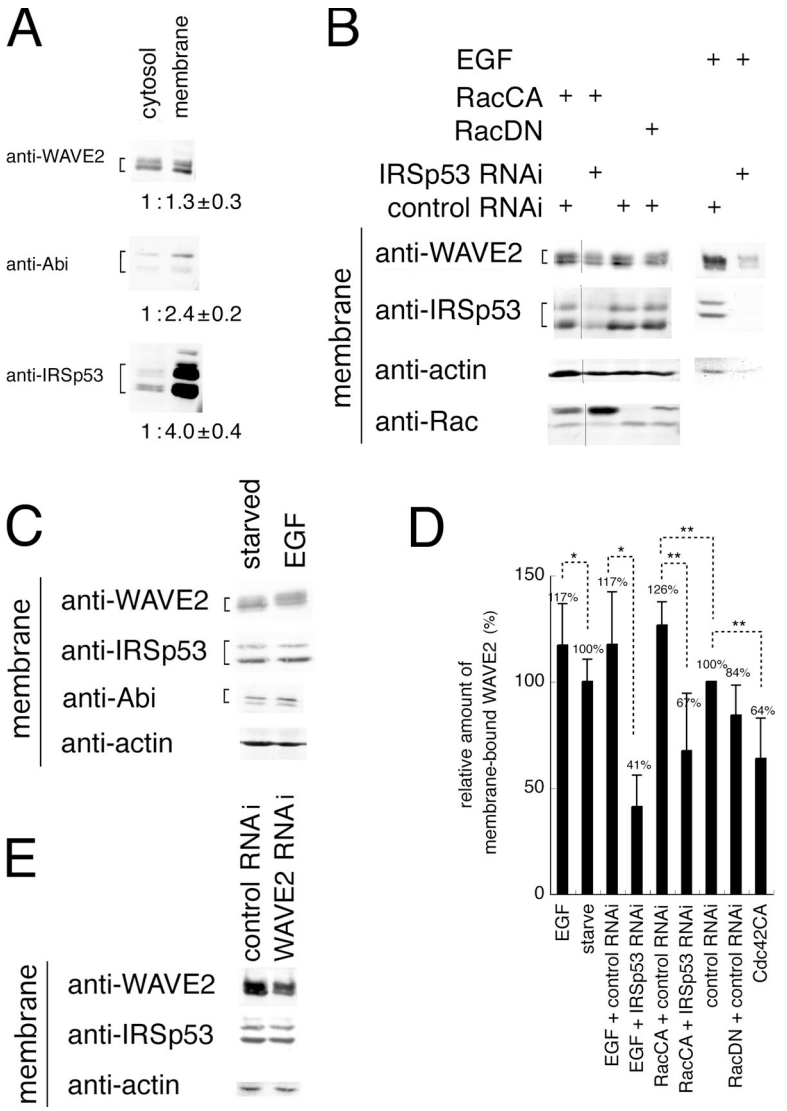

Figure 3. **Role of IRSp53 in WAVE2 localization.** (A–D) Cells were fractionated by ultracentrifugation, and the proteins in each fraction were analyzed by Western blotting. (A) Proteins in membrane and cytosol fractions of serum-starved A431 cells. The ratios of the protein levels were examined by densitometry and expressed with SD. (B) Proteins in the membrane fraction of A431 cells transfected with expression vectors for constitutively active Rac (Rac CA), dominant-negative Rac (Rac DN), control RNAi, and/or IRSp53 RNAi pSuper vector. Stealth RNAi was applied for cells treated with EGF. (C) Proteins in the membrane fraction of EGF-stimulated or unstimulated A431 cells. (D) Quantification of WAVE2 in the membrane fractions. (E) Proteins in the membrane fraction of EGF-stimulated A431 cells transfected with stealth RNAi targeted to WAVE2. *, $P < 0.005$; **, $P < 0.05$ by *t* test. Error bars represent SD.

Other WASP family proteins, including N-WASP and WAVE1, were not identified in the WAVE2 complex (Fig. 4, A and B).

Proteins coeluted with WAVE2 did not differ significantly in response to EGF stimulation. Because WAVE2 in the membrane was increased only 17% upon EGF stimulation (Fig. 3), a lack of difference in the WAVE2 complex before and after stimulation may be reasonable. The expression of Rac CA or Rac DN also did not cause significant change in the WAVE2 complex (unpublished data). Mass spectrometry and Western blotting identified PIR121/Sra1, Nap1/p125NckAP1, and Abi1/Abi2/E3B1 in all WAVE2 complex preparations as reported previously (Innocenti et al., 2004; Steffen et al., 2004; unpublished data). We also identified IRSp53 comigrating with Abi1 and IgG in the Triton X-100 fraction only by SDS-PAGE independently of EGF stimulation (Fig. 4 B, bottom).

From the band intensity in Coomassie brilliant blue–stained gels (unpublished data), the molar ratio of Abi, Nap1, or Sra1 to FLAG-WAVE2 was determined to be ~0.5–0.6 (Fig. 4 C), suggesting the presence of monomeric WAVE2 upon FLAG-WAVE2 expression. Importantly, the amounts of PIR121/Sra1, Nap1, and Abi in the WAVE2 complex were consistently independent of stimuli or subcellular localization, indicating stable formation of the WAVE2 complex.

The band corresponding to IRSp53 was not apparent in silver-stained gels; there was no apparent difference in band intensities between the Triton X-100 and the cytosolic WAVE2 complex in silver-stained gels despite the detection of IRSp53 only in the Triton X-100 fraction by Western blotting. The molar ratio of IRSp53 to WAVE2 in the Triton X-100 fraction of purified WAVE2 complex from cells was 0.0005 by quantitative Western blotting with standard proteins purified from baculovirus (unpublished data). Because the ratio of cytosolic to membrane WAVE2 was 1.3, the molar ratio of IRSp53 to WAVE2 in the membrane was estimated to be 0.001, suggesting a transient interaction between IRSp53 and WAVE2.

Measurement of the binding constant and the intracellular concentrations of WAVE2 and IRSp53

Abi1 and IRSp53 bind to WAVE2 via the coiled-coil region of Abi1 and the SH3 domain of IRSp53 (Miki et al., 2000; Echarri et al., 2004). We measured the dissociation constant

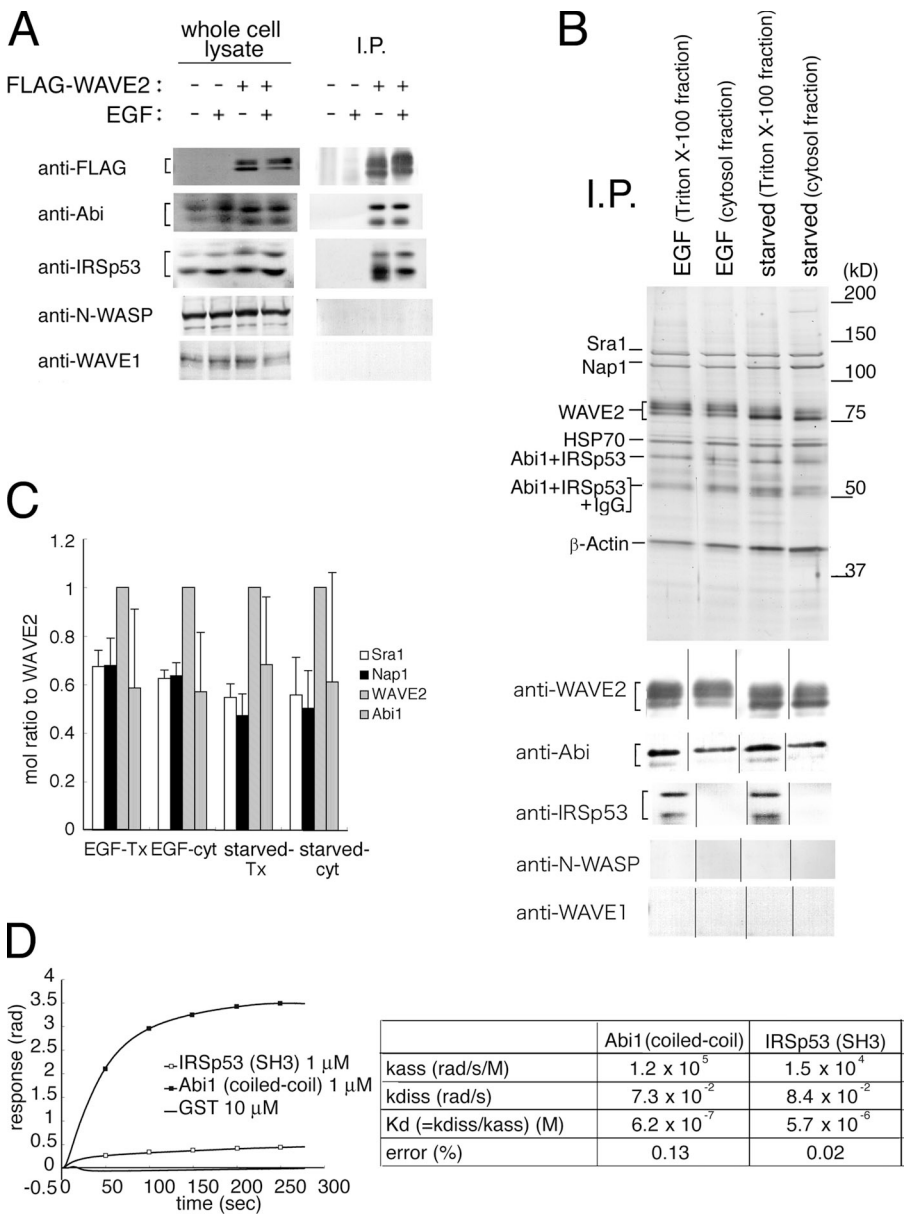

	Abi1 (coiled-coil)	IRSp53 (SH3)
kass (rad/s/M)	1.2×10^{5}	1.5×10^{4}
kdiss (rad/s)	7.3×10^{-2}	8.4×10^{-2}
Kd (=kdiss/kass) (M)	6.2×10^{-7}	5.7×10^{-6}
error (%)	0.13	0.02

Figure 4. **WAVE2 complex purified from A431 cells.** (A) FLAG-tagged WAVE2 was immunoprecipitated from A431 cells stably expressing FLAG-WAVE2 or from control vector–transfected cells by FLAG affinity immunoprecipitation (IP). Specific association was examined by Western blot analysis. (B) WAVE2 complex was purified from A431 cells stably expressing FLAG-WAVE2 by FLAG affinity immunoprecipitation. The Triton X-100 fraction indicates WAVE2 from both the cytosol and membrane fractions, and the cytosol fraction indicates WAVE2 from the cytosol fraction alone. WAVE2 complex from EGF-treated cells (EGF) or untreated cells (starved) are shown in silver-stained gels. The orders of the samples of Western blots are arranged to fit the order of the samples of silver-stained gels. (C) Molar ratio of the components of the WAVE2 complex shown in B. Molar ratio was determined as the band intensity of Coomassie brilliant blue–stained gels (not depicted) divided by molecular weight. Tx, Triton X-100; cyt, cytosol. (D) The dissociation constants (Kd) of the indicated domains to WAVE2 were determined using a dual polarization interferometer. The representative response curves (top) used for the calculation of Kd (bottom) are shown. Error bars represent SD.

(Kd) between full-length WAVE2 and the coiled-coil region of Abi1 (aa 6–124) or between full-length WAVE2 and the SH3 domain of IRSp53 (aa 363–521) with a dual polarization interferometer, and the Kds were determined to be 0.6 and 5.7 μM, respectively (Fig. 4 D).

We then measured the intracellular concentration of WAVE2 or IRSp53 by quantitative Western blotting with purified WAVE2 or IRSp53 as standards. WAVE2 concentration in whole cell lysates was 30–50 nM, whereas that of IRSp53 was 150–300 nM. Given the Kd of 5.7 μM for WAVE2 and IRSp53, only 2.5 nM WAVE2 was associated with IRSp53 in solution at WAVE2 and IRSp53 concentrations of 50 and 300 nM, respectively. Therefore, the Kd value between IRSp53 and WAVE2 suggests that these two proteins associate with the aid of other molecules such as Rac or PIP_3 or in a restricted location such as the cell membrane. Even if WAVE2 and IRSp53 associate under limited situations, the 10-fold difference in Kd values appears to explain the lesser amount of IRSp53 in the aforementioned purified WAVE2 complex. Three washes in 10-fold volumes of buffer will result in a 1,000-fold difference in protein amount.

Similar activity of the WAVE2 complex to that of the WAVE2 monomer

Most WAVE2 molecules are reported to complex with Sra1/PIR121, Nap1, and Abi1. We fractionated lysates of control A431 cells or cells expressing FLAG-tagged WAVE2 in a 3–30% sucrose gradient. Most of the WAVE2 in control cells formed a protein complex, but a small population of monomeric WAVE2 was found (Fig. 5 A). Approximately half of the WAVE2 in cells stably expressing FLAG-WAVE2 was monomeric and not associated with Abi1 (Fig. 5 B). Therefore, the presence of monomeric WAVE2 in cells expressing FLAG-WAVE2 is caused by the ectopic expression of WAVE2. We also created a WAVE2 knockout MEF cell line stably expressing FLAG-WAVE2 in

amounts similar to that of wild-type cells (Yamazaki et al., 2005). Most of the WAVE2 in WAVE2 knockout cells expressing FLAG-WAVE2 formed a complex (Fig. 5 C) in a manner similar to wild-type cells (unpublished data). In all of the lysates we prepared, IRSp53 was not coeluted with WAVE2 (Fig. 5, A–C), indicating that IRSp53–WAVE2 association is very weak or transient. As reported previously, Abi1 was essential for WAVE2 complex formation because RNAi of Abi1 increased the amount of monomeric WAVE2 compared with that of the WAVE2 complex (Fig. 5 D). In contrast, RNAi of IRSp53 did not significantly affect WAVE2 complex assembly (Fig. 5 E and Fig. S1 C).

We next examined the stability of the WAVE2 complex by sequential sucrose gradient. The high molecular weight fraction of the FLAG-WAVE2 preparation obtained from a sucrose gradient was further subjected to another sucrose gradient (Fig. 5 E), showing that the WAVE2 complex was stable without any dissociation of the components in the second sucrose gradient. We then examined the dependence of protein complex formation on WAVE2 localization or EGF stimulation. The amount of WAVE2 in the smaller molecular weight fraction was not increased upon stimulation (Fig. 5, F–I; and Fig. S3, available at http://www.jcb.org/cgi/content/full/jcb.200509067/DC1). A small population of IRSp53 was found in the WAVE2 complex fraction and monomeric WAVE2 fraction, but it appeared to dissociate during fractionation (Fig. 5, F and H). Differences in the localization of WAVE2 (cytosolic or Triton X-100) did not result in differences in the amounts of the two populations of WAVE2 (Fig. 5, F–I; and Fig. S3). We added GTPγS-loaded Rac alone (Fig. 5 J and Fig. S3) or a combination of GTPγS-loaded Rac, IRSp53, and PIP_3-containing liposomes (Fig. 5 K and Fig. S3) to cell-purified WAVE2. However, no significant increase in WAVE2 in the smaller molecular weight fraction was observed.

To examine the dependence of activities on WAVE2 complex formation, we analyzed the activity of each sucrose gradient fraction from Triton X-100 fractions of serum-starved cells in Arp2/3-mediated actin polymerization assays. As a control, actin polymerization was induced in sucrose gradients prepared in the absence of protein. Increased sucrose concentration decreased the rate of actin polymerization, but the maximum actin polymerization achieved was not altered (Fig. 5 L). When the rate of actin polymerization of each fraction was normalized to that induced by Arp2/3 alone, WAVE2 protein concentration, as determined by Western blotting, was associated with Arp2/3 activation (Fig. 5, M and N). Therefore, actin polymerization between monomeric WAVE2 and the WAVE2 complex did not differ significantly.

High activity of WAVE2 complex from the membrane fraction independent of protein complex formation

Because we did not detect significant differences in Arp2/3 activation between the two WAVE2 populations, we examined the activity of the entire WAVE2 elution. We did not detect any significant alterations in actin polymerization in WAVE2 protein complexes alone (unpublished data). When we added purified Arp2/3, WAVE2 complex from various preparations showed Arp2/3 complex activation (Fig. 6, A and B). WAVE2 complex from the Triton X-100 fraction showed greater Arp2/3 complex activation than that from the cytosol fraction (Fig. 6 A). To assess differences in activity more quantitatively, we determined concentration-dependent activation curves for WAVE2 complexes from various preparations (Fig. 6 B). From these curves, we confirmed that WAVE2 complex from the Triton X-100 fraction had greater activity than that from the cytosol fraction. WAVE2 complex activity from the Triton X-100 fraction was similar to that of the VCA domain of WAVE2 (Fig. 6 B). EGF stimulation did not alter WAVE2 activity. Thus, cytosolic WAVE2 was not fully activated but membrane WAVE2 was. Because WAVE2 from the Triton X-100 fraction was fully active and WAVE2 in the protein complex had similar activity to that of WAVE2 not in the complex (Fig. 5 H), WAVE2 in the protein complex may be fully activated.

We also measured the activity of the WAVE2 complex in MEFs. Almost all of the WAVE2 was complexed (Fig. 5 C). The activity of the WAVE2 complex prepared from the Triton X-100 fraction was also higher than that of the cytosolic WAVE2 complex, and no significant difference in the activities was induced by EGF stimulation (Fig. 6 C).

IRSp53-dependent activation of the WAVE2 complex

To determine the absence or presence of IRSp53, we performed RNAi experiments to decrease IRSp53 expression. WAVE2 complex purified from the Triton X-100 fraction of cells with decreased IRSp53 expression by vector-based RNAi or by siRNA showed decreased Arp2/3 complex activation (Fig. 6, D and E; and not depicted). Restoration of IRSp53 in IRSp53 RNAi cells restored WAVE2 activity (unpublished data). The activity of the cytosolic WAVE2 complex was not altered (unpublished data), and the WAVE2 complex showed no detectable changes in silver-stained gels and in Western blot analysis in response to RNAi of IRSp53 (Fig. S1 C).

We next examined whether exogenous IRSp53 activates the cytosolic WAVE2 complex. The addition of a 10-fold molar excess of purified IRSp53 to the cytosolic WAVE2 complex activated the Arp2/3 complex (Fig. 6 F), strongly indicating that IRSp53 activates WAVE2 at the membrane.

Rac-, IRSp53-, and PIP_3-dependent activation of WAVE2 independent of protein complex formation

To confirm the activation of WAVE2 by IRSp53, we prepared recombinant proteins (Fig. S4, available at http://www.jcb.org/cgi/content/full/jcb.200509067/DC1). We examined whether IRSp53 was able to activate recombinant WAVE2 alone or the reconstituted WAVE2 complex (Fig. S4). We also examined the effects of PIP_3-containing liposomes or control liposome composed of phosphatidylcholine (PC) and PI and that of lipidated Rac. Recombinant WAVE2 alone was activated by IRSp53 in the presence of GTPγS-loaded Rac and PIP_3-containing PC/PI liposomes (Fig. 7, A and C). However, activation was not observed with Cdc42 or with liposome lacking

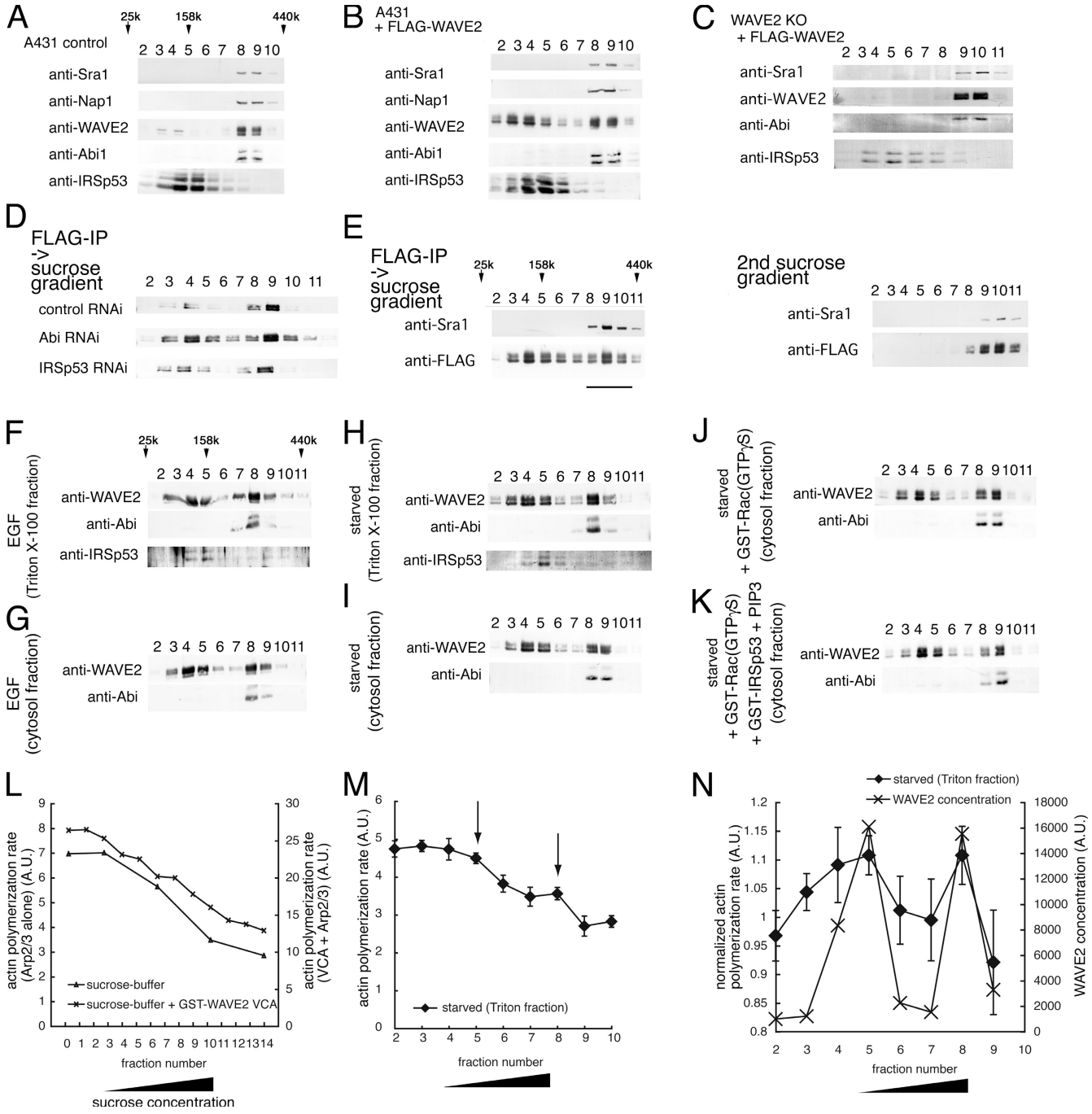

Figure 5. **Fractionation of cell lysate and purified WAVE2 from A431 cells by sucrose gradient.** (A–C) Cell lysates of control A431 cells (A), A431 cells stably expressing FLAG-tagged WAVE2 (B), and WAVE2 knockout MEF stably expressing FLAG-tagged WAVE2 (C) were fractionated by molecular weight in a 3–30% sucrose gradient, and each fraction was visualized by Western blotting. (D–K) Purified WAVE2 from A431 cells stably expressing FLAG-tagged WAVE2 was fractionated. (D) WAVE2 purified from the Triton X-100 fraction of pSuper vector–transfected cells of control, IRSp53, or Abi1 RNAi. (E) Sequential sucrose gradient fractionation. WAVE2 purified from the Triton X-100 fraction was fractionated, and the high molecular weight fraction (fraction 8–10) was further fractionated. Bar indicates the fractions that were used in the second sucrose gradient. (F) WAVE2 purified from the Triton X-100 fraction of EGF-treated cells. (G) Cytosol fraction of EGF-treated cells. (H) Triton X-100 fraction of serum-starved cells, and (I) cytosol fraction of serum-starved cells. (J and K) WAVE2 from the cytosol fraction of serum-starved cells was incubated with GTPγS-loaded Rac (J) or GTPγS-loaded Rac, IRSp53, and PIP_3 (K). (L and M) Activities of the WAVE2 monomer and WAVE2 complex were compared. (L) Sucrose gradient in the absence of protein was also used as a control. The axis of actin polymerization rate for VCA + Arp2/3 is on the right, and that for Arp2/3 alone is on the left. (M) Each sucrose gradient fraction of WAVE2 from the Triton X-100 fraction of serum-starved cells was analyzed for Arp2/3 complex activation with 50 nM of purified Arp2/3 complex and 2 μM of 10% pyrene-labeled actin. The rate of actin polymerization at 10% polymerization was determined and plotted relative to fraction number. Arrows indicate the peak fraction of the activity of the Arp2/3 complex activation in N. (N) The value of slope in M was normalized to the value of Arp2/3 alone in L as 1 (left axis) and was plotted with WAVE2 concentration determined by Western blotting followed by densitometry (right axis). Error bars represent SD.

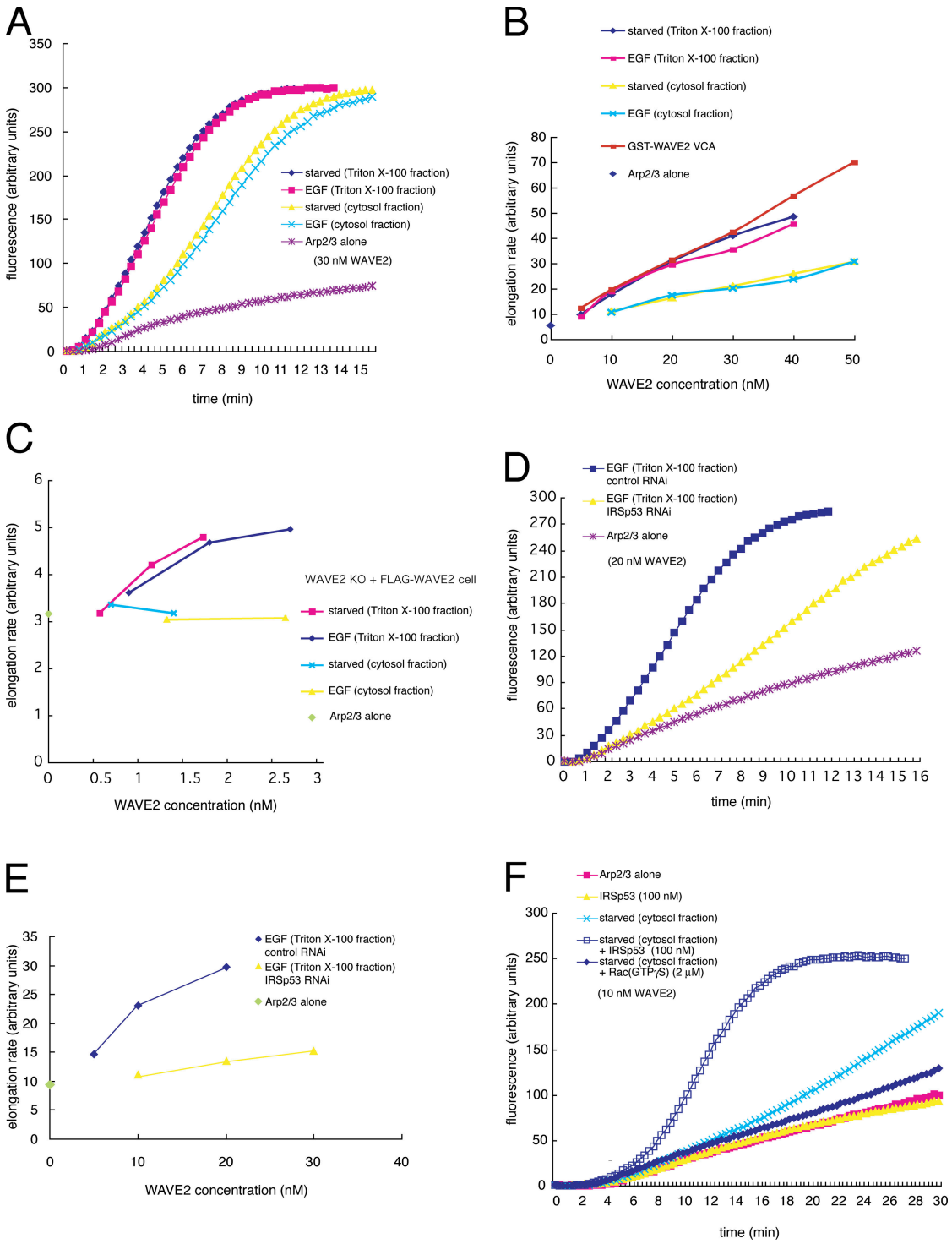

Figure 6. **Arp2/3 complex activation by the WAVE2 complex.** (A and D) WAVE2 complex purified from the Triton X-100 or cytosol fraction with (EGF) or without stimulation (starved) of A431 cells (A) and from the Triton X-100 fraction of control or IRSp53 RNAi-treated cells (D) was analyzed for Arp2/3 complex activation ability with 50 nM Arp2/3 complex and 2 μM of 10% pyrene-labeled actin. Actin polymerization was monitored by pyrene fluorescence. The VCA fragment of WAVE2 was also analyzed for concentration-dependent activation of the Arp2/3 complex. (B and E) Dose-response curves for A and D show the change in filament elongation rate as a function of increasing concentrations of WAVE2 complex. Elongation rate was determined by the slope of fluorescence change at 15% actin polymerization. (C) Dose-response curves show the change in filament elongation rate as a function of increasing concentrations of WAVE2 complex purified from the Triton X-100 or cytosol fraction with (EGF) or without stimulation (starved) of WAVE2 knockout MEFs stably expressing FLAG-WAVE2. (F) WAVE2 complex purified from the cytosol fraction was mixed with recombinant IRSp53 or GTPγS-loaded Rac, and Arp2/3 complex activation was measured as in A.

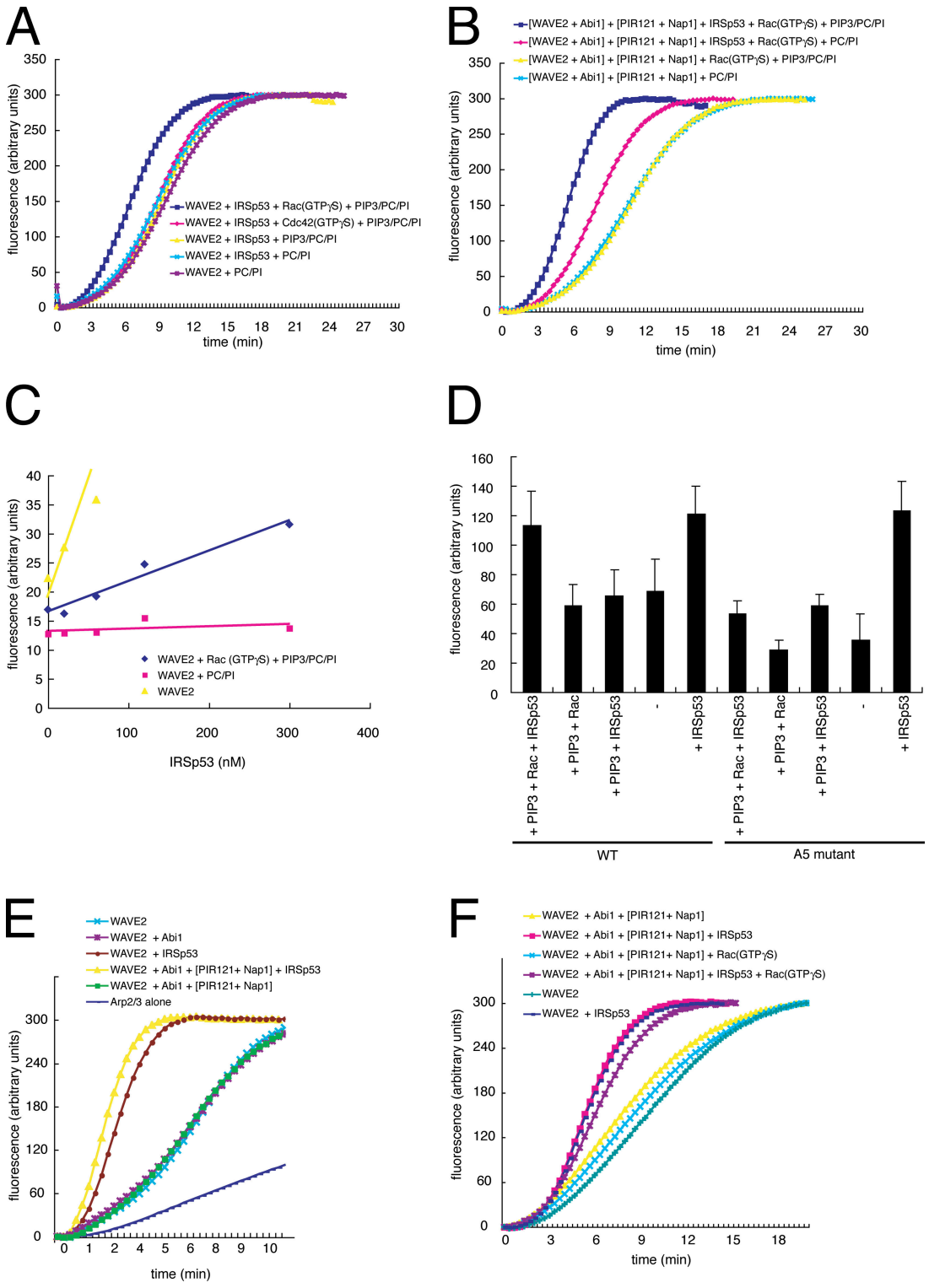

Figure 7. **Rac- and PIP_3-dependent actin polymerization mediated by IRSp53 and WAVE2.** (A) 40 nM of purified recombinant WAVE2 was preincubated with 60 nM of recombinant IRSp53, 300 nM GTPγS-loaded Rac, 300 nM GTPγS-loaded Cdc42, 8 μM PIP_3-containing PC/PI liposomes (PIP_3/PC/PI), and/or PC/PI liposomes. Arp2/3 complex activation was determined with 50 nM Arp2/3 complex and 2 μM of 10% pyrene-labeled actin. (B) 40 nM of purified recombinant WAVE2 coexpressed and copurified with Abi1 that was incubated with recombinant PIR121 copurified with 250 nM Nap1. Rac-, PIP_3-, and IRSp53-dependenent Arp2/3 activation was examined as in A. (C) Concentration response of filament elongation rate dependent on IRSp53 concentration. Purified recombinant WAVE2 was incubated with various concentrations of IRSp53 in the absence or presence of PIP_3/PC/PI liposome and GTPγS-loaded Rac or PC/PI liposomes alone. (D) Purified recombinant wild-type or PIP3 binding-defective A5 mutant of WAVE2 was incubated with IRSp53 in the absence or presence of PIP_3/PC/PI liposome and GTPγS-loaded Rac. Filament elongation rate is shown with SD (error bars). (E) 100 nM of purified recombinant WAVE2, 250 nM Abi1, PIR121 copurified with 250 nM Nap1, and/or 500 nM IRSp53 were mixed, and Arp2/3 complex activation was measured in the absence of liposomes. (F) Effect of 15 μM GTPγS-loaded Rac on Arp2/3 activation in the absence of liposomes.

PIP_3, indicating that PIP_3, Rac, and IRSp53 are required for the activation of WAVE2.

We also examined the activation of the reconstituted WAVE2 complex. Abi1, Nap1, and PIR121 did not show the activation of WAVE2 (Fig. 7 B). Lack of PIP_3, Rac, and/or IRSp53 decreased the activation of WAVE2. Cdc42 failed to activate the reconstituted WAVE2 complex in the presence of IRSp53 and PIP_3-containing liposomes (unpublished data). PIP_3-containing liposomes alone were not sufficient for activation of the WAVE2 complex. Rac did not activate the reconstituted WAVE2 in the presence of liposomes (Fig. 7 B).

To confirm the PIP_3- and Rac-dependent activation of WAVE2 by IRSp53, various concentrations of IRSp53 were examined (Fig. 7 C). In the presence of PC/PI, IRSp53 did not activate WAVE2. However, in the presence of Rac and PIP_3/PC/PI, IRSp53 activated WAVE2 in a concentration-dependent manner. Thus, Rac requires IRSp53 to activate WAVE2 in the presence of liposomes. The A5 mutant of WAVE2, which is defective in PIP_3 binding (Oikawa et al., 2004), failed to be activated by IRSp53 in the presence of Rac and PIP_3-containing liposome (Fig. 7 D).

Interestingly, IRSp53 alone activated WAVE2 in the absence of liposomes or the PIP_3-binding ability of WAVE2 (Fig. 7, C–E). Indeed, the activation of WAVE2 by IRSp53 was much stronger in the absence of liposomes (Fig. 7 C). Thus, liposomes may titrate out IRSp53 from WAVE2 by a nonspecific IRSp53–lipid association. PIP_3 and Rac may then aid the association between IRSp53 and WAVE2 in the presence of liposomes.

In the absence of liposomes, Abi1, Nap1, and PIR121 showed no significant WAVE2 activation (Fig. 7 F). The addition of Rac to WAVE2 alone or the reconstituted WAVE2 complex did not affect actin polymerization in the absence of liposomes (Fig. 7 F and not depicted).

IRSp53 binds to lipid via the RCB domain

PIP_3-dependent activation of WAVE2 by Rac and IRSp53 indicates that IRSp53 also binds to lipids. The crystal structure of the NH_2-terminal domain of IRSp53, termed the IMD or RCB domain, has been reported previously (Millard et al., 2005). The overall surface of the IMD is positively charged, suggesting that the IMD binds to the electronegative inner leaflet of the cell membrane. We determined the binding of the RCB domain, the shorter fragment of the IMD, to lipids by ELISA (Oikawa et al., 2004), in which various lipids were coated onto plates. The RCB domain bound to almost all of the lipid species, with increased binding corresponding to increased negative charges (Fig. 8 B). The RCB domain bound strongly to phosphatidylserine or weakly to PI, which are abundant lipids of the cell membrane (Fig. 8 B). The affinity of the RCB domains to various lipids indicated the nonselective binding of the RCB domain to the membrane. In the liposome cosedimentation assay, where bound proteins to the liposome were examined, no difference in affinity was observed between PIP_3-containing liposomes and PIP_3-lacking liposomes (Fig. 8 C and not depicted). Without liposome, only a trace amount of RCB protein was found in the precipitates (Fig. 8 D). Therefore, although RCB domain bound to negatively charged lipids, there was no selective binding of the RCB domain to PIP_3 or other phosphoinositides. IRSp53 appears to bind to the cell membrane via electrostatic interactions between the RCB domain and membrane.

Rac- and PIP_3-dependent association between WAVE2 and IRSp53 in the presence of liposomes

We next examined the association of Rac, IRSp53, and WAVE2 with PIP_3-containing liposomes. Recombinant IRSp53 bound to PIP_3/PC/PI liposomes (Fig. 9, A–C) but also bound to PC/PI liposomes at this concentration. Rac purified from Sf9 cells also associated with liposomes, presumably through lipid modification (Fig. 8, A and B; Hall, 1998). WAVE2 alone also bound to PIP_3 (Oikawa et al., 2004), but in the presence of both activated (GTPγS loaded) Rac and IRSp53, the association of WAVE2 with PIP_3-containing liposomes increased fivefold (Fig. 9, A and C). Importantly, the increase in WAVE2 association in the presence of liposomes was not observed with GTPγS-loaded Cdc42, GDP-loaded Rac, or liposomes lacking PIP_3 (Fig. 9, A–C). High molecular weight WAVE2 complex prepared by

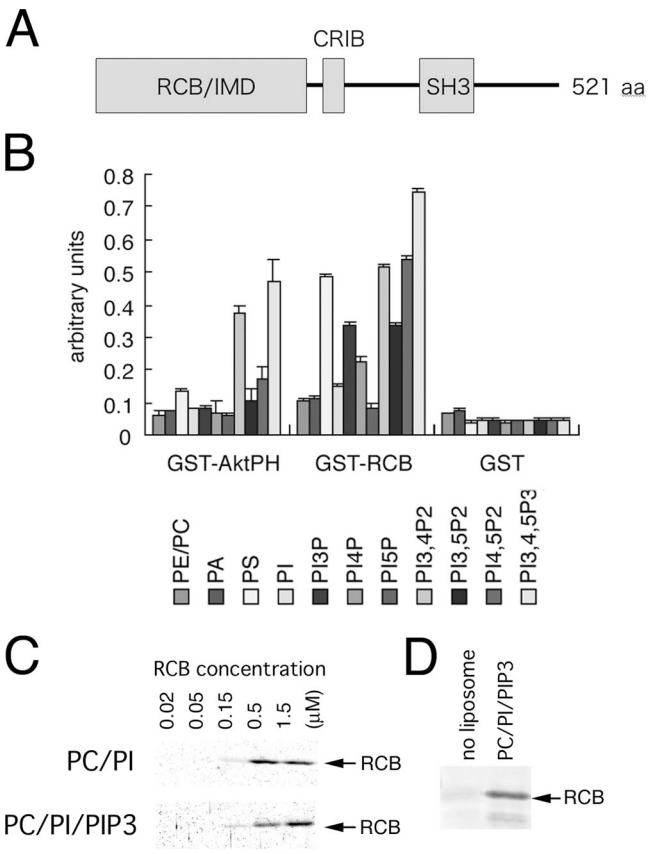

Figure 8. **Association of IRSp53 with lipids.** (A) Domain structure of IRSp53. (B) Quantification of the phosphoinositide-binding abilities of the RCB domain. ELISA was performed with GST as a negative control and GST-AktPH as positive controls. 1.0 μg ml^{-1} GST-tagged proteins were overlaid on lipid vesicles (PE/PC/PIXP, PA, or phosphatidylserine [PS] = 1:1:0.2 μg). Error bars represent SD of at least three independent experiments. PA, phosphatidic acid; PE, phosphatidyl ethanolamine. (C) Liposome binding by the RCB domain. Liposomes (PC/PI/PIP_3 = 48:48:4 or PC/PI = 50:50) were mixed with the RCB protein at the indicated concentrations. The proteins that cosedimented with the liposomes were visualized. (D) Negative control of C without liposome at a 1.5-μM RCB concentration.

sucrose gradient from A431 cells stably expressing FLAG-WAVE2 also bound to PIP_3 in the presence of IRSp53 and Rac (Fig. 9 E). Thus, PIP_3 and Rac appear to greatly enhance the association between IRSp53 and WAVE2 or the WAVE2 complex on liposomes or cell membrane. The actin polymerization assay on PIP_3- or PI-coated beads confirmed the PIP_3-dependent association and activation of WAVE2 (Fig. S5, available at http://www.jcb.org/cgi/content/full/jcb.200509067/DC1).

Discussion

In this study, we showed that IRSp53 is involved for the activation of WAVE2 in the membrane fraction of cells. IRSp53 was significantly concentrated in the membrane fraction, whereas WAVE2, Abi1, Nap1, and Sra1 were not. We also showed that both the WAVE2 complex from cells and the reconstituted WAVE2 complex could be fully active. IRSp53 enhanced the activation of WAVE2 in the absence of liposomes. However, Rac possesses a lipid modification and exists at the membrane, and IRSp53 induced the Rac-dependent activation of WAVE2 or WAVE2 complex only in the presence of PIP_3-containing liposomes. Therefore, PIP_3 at the membrane is essential for the Rac-dependent association of IRSp53 and WAVE2. In the presence of liposomes lacking PIP_3, the weak binding of WAVE2 to liposomes inhibited its activation by IRSp53. Cdc42, another small GTPase that binds to IRSp53, weakened the association between IRSp53 and WAVE2.

Regulation of WAVE2 and actin cytoskeletal reorganization

Our experiments did not detect differences in WAVE2 activity in Arp2/3 activation between no stimulation, EGF stimulation

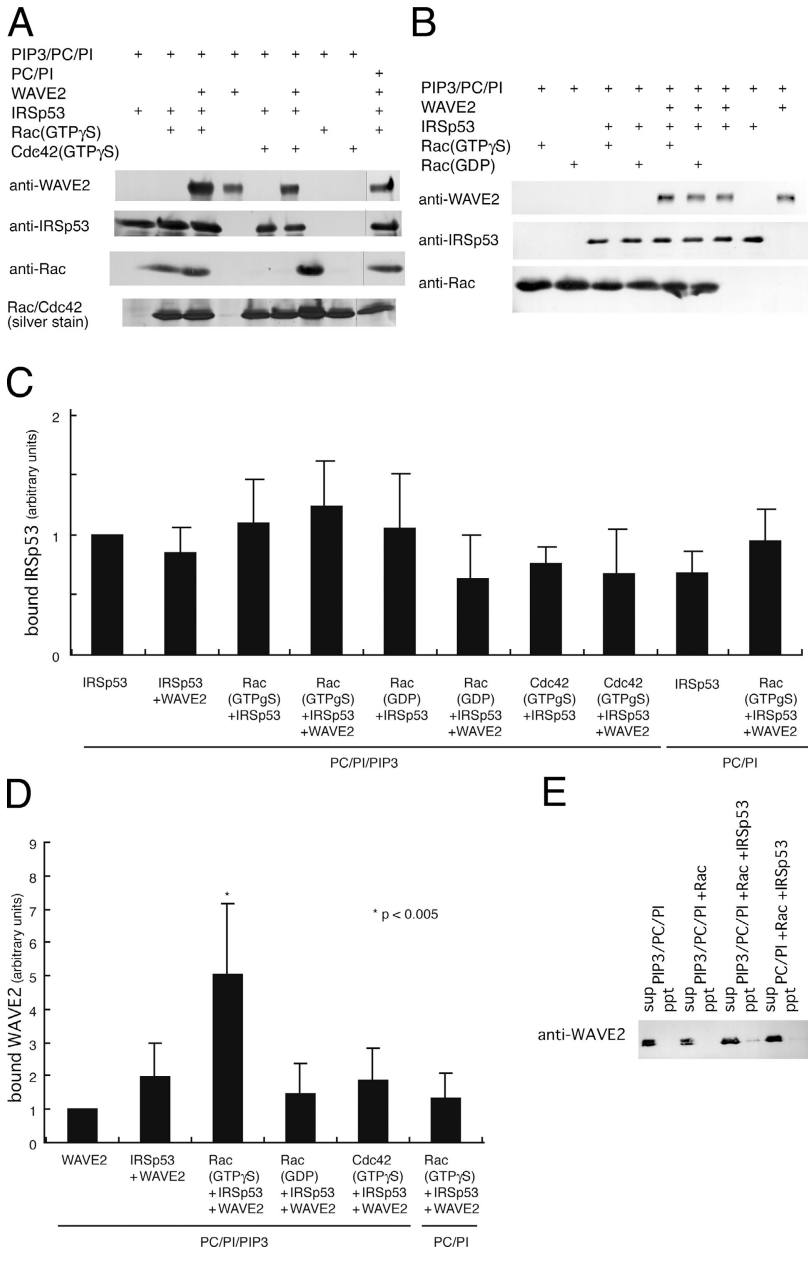

Figure 9. **Rac- and PIP_3-dependent actin polymerization mediated by IRSp53 and WAVE2 on PIP_3.** (A and B) Protein–lipid association was monitored by cosedimentation assay. Cosedimented proteins with liposomes with or without PIP_3 were examined by Western blot analysis. PIP_3, WAVE2, IRSp53, Rac, and Cdc42 were included at concentrations of 8 μM, 60 nM, 60 nM, 300 nM, and 300 nM, respectively. (C and D) Quantification of proteins bound to liposomes was determined by densitometry for IRSp53 (C) and WAVE2 (D). Error bars represent SD. (E) Lipid association of the WAVE2 complex purified from the high molecular weight fraction of sucrose gradient fractionation from A431 cells was monitored by cosedimentation assay. Cosedimented proteins with liposomes containing or lacking PIP3 were examined by Western blot analysis. GTPγS-loaded Rac and IRSp53 were added, and their effects were examined. sup, supernatant; ppt, precipitate.

(Fig. 6), and stimulation in response to the expression of Rac CA (not depicted). The activity of WAVE2 from MEFs was not significantly increased upon stimulation (Fig. 6 C), suggesting that overall WAVE2 activity remains constant before and after stimulation.

When we consider the relationship between membrane localization and activation of WAVE2, EGF stimulation or expression of Rac CA induced only a 15–20% increase in membrane-bound WAVE2 in both A431 cells and MEFs (Fig. 3 and not depicted), and membrane-localized WAVE2 comprised ~60% of WAVE2 in Triton X-100 preparations (Fig. 3). Thus, only an ~10% increase in membrane WAVE2 in the Triton X-100 fraction appears to occur upon EGF stimulation. If EGF stimulation activates WAVE2 by inducing the membrane translocation of WAVE2, it may be too small to be detected in actin polymerization assays with WAVE2 prepared from whole cells.

Possible regulation of WAVE2 by localization via formation of the WAVE2 complex and enhancement of its activity by IRSp53

We did not detect differences in WAVE2 activity from cells, as discussed in the previous section, but we were able to reconstitute Rac-dependent WAVE2 activation and found that IRSp53 associated with the membrane. IRSp53 possesses an NH_2-terminal RCB domain that is also called the IMD. Electrostatic interaction may account for the nonspecific binding of IRSp53 to the membrane (Fig. 8). Rac is also lipidated, and activated Rac is thought to function at the membrane. Therefore, PIP_3 production may simultaneously activate Rac and recruit WAVE2. Because IRSp53 bound to the membrane without specific binding to phosphoinositides, IRSp53 is thought to constitutively bind to the membrane. Activated Rac may recruit IRSp53 to sites of PIP_3 production, where WAVE2 is also recruited. Thus, PIP_3 production may increase the possibility of IRSp53–WAVE2 association at the membrane, resulting in membrane protrusion.

Kinetic analysis and sucrose gradient fractionation revealed that the association of IRSp53 and WAVE2 is very transient. IRSp53 was copurified with WAVE2, but during sucrose gradient fractionation, the majority of IRSp53 appeared to dissociate (Fig. 5). This transient association between IRSp53 and WAVE2 may be involved in the signal-dependent activation of WAVE2. Recently, Tiam1, a Rac guanine nucleotide exchange factor, was reported to enhance the association between IRSp53 and WAVE2 (Connolly et al., 2005). Although we failed to detect Tiam1 in the WAVE2 complex by Western blotting, presumably because of indirect association (unpublished data), proteins such as Tiam1 may participate in the efficient activation of WAVE2.

In contrast to the association of IRSp53 with WAVE2, the WAVE2 complex was very stable, at least in vitro. As reported earlier, Sra1/PIR121, Nap1, and Abi1 binds to Rac, Nck, and Abl, respectively (Eden et al., 2002; Echarri et al., 2004; Innocenti et al., 2004; Steffen et al., 2004). We did not observe the dissociation of the WAVE2 complex upon the addition of Rac or Nck or upon simultaneous addition of IRSp53, PIP_3, and Rac (Fig. 5 and not depicted). Phosphorylation of WAVE2 by Abl has also been reported to play a role in WAVE2 activation (Leng et al., 2005). However, we did not detect any difference in WAVE2 activity upon EGF stimulation in the presence or absence of STI-571, an Abl inhibitor (unpublished data). It has also been reported that Abl is involved in Rac activation and that ruffle formation downstream of Rac is independent of Abl family kinase activity (Sini et al., 2004). However, Abl-mediated phosphorylation of WAVE2 may be involved in other cells. In our experiments, the knockdown of IRSp53 did not induce defects in lamellipodium formation as severe as those induced by the knockdown of Abi1 (Figs. 1 and 2, and Video 1). WAVE2 is essential for the invasion of epithelial cells by *Salmonella*, and increased IRSp53 binding to WAVE2 was reported upon *Salmonella* infection (Shi et al., 2005). However, IRSp53 was not essential for the invasion itself. These results indicate that WAVE2 is regulated mainly by its localization via formation of the WAVE2 complex (Innocenti et al., 2004; Steffen et al., 2004). Therefore, IRSp53 may optimize WAVE2 activity by enhancing its activation of the Arp2/3 complex.

In a previous study of the WAVE1 protein complex in the brain, dissociation of WAVE1 from the partial protein complex of Abi, Nap1, and Sra1/PIR121 was observed upon incubation with Rac or Nck, and the WAVE1 complex alone was substantially inactive, suggesting the activation of WAVE1 upon dissociation from the complex (Eden et al., 2002). We have also observed that cytosolic WAVE2 had less activity than membrane-bound WAVE2 from A431 cells and MEFs. Also, we found that the WAVE2 complex, both reconstituted and purified from cells, can be fully active without dissociation of the complex. The reason for this discrepancy is not known, but it may be caused by different WAVE complex purification protocols; Eden et al., (2002) used ammonium sulfate precipitation of the cytosolic fraction of the brain to purify WAVE1, whereas we immunoprecipitated WAVE2 directly from cell lysates. Protocol differences may result in the loss of unidentified complex components that activate WAVE2 in our preparations. Alternatively, differences between WAVE1 and WAVE2 may be involved.

Materials and methods

Cells and purification of the WAVE2 complex

A431 cells were transfected with FLAG-tagged WAVE2 in pCMV-Tag 2 (Stratagene) or with vector alone. FLAG-tagged WAVE2 is functional because the transfection of FLAG-tagged WAVE2 into WAVE2 knockout cells eliminated WAVE2 deficits. After selection with G418, cells with stable FLAG-WAVE2 expression were grown. These cells did not show any significant change in growth or appearance compared with vector-transfected cells or parental cells. The amount of FLAG-WAVE2 expression was similar to the amount of endogenous WAVE2. 10^6 cells were plated onto 15-cm dishes and cultured for 5 d. After serum starvation overnight, some cultures were stimulated with EGF. To purify the WAVE2 complex from the cytosol (cytosol fraction), cells were harvested in buffer A containing 20 mM Tris-HCl, pH 7.5, 5 mM EDTA, 150 mM NaCl, 5 mM NaF, 1 mM Na_3VO_4, 1 mM PMSF, 10 μg/ml aprotinin, and 10 μg/ml leupeptin. To purify the WAVE2 complex, including that from the membrane fraction (Triton fraction), cells were harvested in buffer A supplemented with 1% Triton X-100 and 10% glycerol. Cells were sonicated and clarified by centrifugation at 20,000 *g* for 20 min. The resulting supernatant was mixed with FLAG-agarose affinity gel (Sigma-Aldrich). After being mixed for 1 h, gels were washed with buffer A supplemented with 0.5% Triton X-100 and 10% glycerol and were washed with buffer XB containing 10 mM Hepes, pH 7.9, 100 mM KCl, 2 mM $MgCl_2$, 0.2 mM $CaCl_2$, and 5 mM EGTA.

FLAG-WAVE2 complex was eluted with buffer XB plus 0.5 mg/ml FLAG peptide (Sigma-Aldrich). The eluted protein was analyzed or processed with sucrose gradient fractionation. 3–30% sucrose gradient was prepared in buffer XB supplemented with 10% glycerol, and the gradient was centrifuged at 200,000 *g* for 15 h. After sucrose gradient, the WAVE2 complex at high molecular weight fraction (typically fraction No. 8–10) was used for further experiments after concentration by the Ultrafree filter (Millipore).

Transfection and RNAi experiments

Cells were transfected with FuGene 6 (Roche). 10^6 cells in 15-cm dishes were cultured for 24 h, and these cells were transfected for 24 h and cultured for 24 h. Cells were then starved overnight and used for assays. RNAi was performed as described previously with pSuper vector (Kurisu et al., 2005) or stealth RNAi (Invitrogen). The sequence of IRSp53 RNAi was GGAGCTGCAGTACATCGAC. Abi1 RNAi was performed as described previously (Steffen et al., 2004). Control RNAi was performed with pSuper vector with a sequence that caused no reduction of protein expression. Transfection efficiency was ∼80% when monitored by transfection with GFP-expressing plasmid. For cotransfection with WAVE2-GFP (Suetsugu et al., 2003), WAVE2-GFP and RNAi vector plasmids were mixed at 1:4 ratios to ensure the cotransfection of GFP-positive cells. Rac G12V and Cdc42 G12V were used as CA Rac and Cdc42, respectively, and were expressed in the pEF-BOS vector (Suetsugu et al., 2003). IRSp53 was tagged with Venus, a brighter variant of GFP (Nagai et al., 2002).

siRNA was performed with stealth RNAi (Invitrogen). The siRNA sequence targeting was as follows: IRSp53 #1, 5′-AGUACUCGGACAAGGAGCUGCAGUA-3′;IRSp53 #2,5′-ACUCGGACAAGGAGCUGCAGUACAU-3′; IRTKS #1, 5′-CAAUCCUGGGCUGCGAAAUUUAAUA-3′; IRTKS #2, 5′-CGUGAAAUAUAUGAACGCAACUCUA-3′; IRTKS #3, 5′-CGUGAAAUAUAUGAACGCAACUCUA-3′; IRTKS #4, 5′-CAAGGAAGCCGAAACGCACUCAAAU-3′; control #1,5′-AGUGGCUAACAGAGGCGUCACAGUA-3′; control #2, 5′-ACUAGACGAAGCGGUACUGAGCCAU-3′; control #3, 5′-CAAGUCCGGCGUAAGUUAAUUCAUA-3′; control #4, 5′-CAAGAAGCCAAACGCUCAACGGAAU-3′; Abi1 #1, HSS115189 (Invitrogen); Abi1 #2, HSS115190 (Invitrogen); and Abi1 #3, HSS115191 (Invitrogen). A431 cells were transfected with 2.6 μl of 20 μM siRNA in 120 μl OPTI-MEM and 1.2 μl LipofectAMINE 2000 reagent (Invitrogen) in 120 μl OPTI-MEM in a six-well plate with 1 ml DME + 10% FCS. After 24 h, a second transfection was performed, and the cells were cultured for 48 h and subjected to RT-PCR or various experiments. The mRNA from RNAi-treated A431 cells was isolated using TRIzol reagent (Invitrogen). A first-strand cDNA was synthesized from the mRNA by the SuperScript First-strand synthesis system for RT-PCR (Invitrogen). The PCR amplification was performed using the first-strand cDNA. Amplification conditions were as follows: 25 cycles of 30 s at 95°C, 30 s at 60°C, 60 s at 72°C, and a final extension of 10 min at 72°C. IRSp53 expression construct that was resistant for RNAi was prepared by g486a and c495a mutations.

Antibodies

Anti-IRSp53 and anti-Abi1 antibodies were raised by immunizing rabbits with full-length IRSp53 and Abi1 proteins purified from *Escherichia coli* as GST fusion proteins. Anti-WAVE2 was raised as described previously (Yamazaki et al., 2003). Anti-GFP antibody was purchased from MBL International Corporation, and anti-FLAG M2 antibody was obtained from Sigma-Aldrich. Cell staining was performed as described previously, and actin filaments were stained with phalloidin (Suetsugu et al., 2003). Cells were then observed by confocal microscopy (Bio-Rad Laboratories). Anti-IRTKS antibody (M051-3) was purchased from MBL International Corporation and was found to be anti-IRSp53 antibody (Fig. S1 B).

Cell fractionation

Cells were harvested in buffer A and sonicated. Lysates were clarified by centrifugation at 3,000 *g* for 30 min to remove nuclei and debris. Supernatants were then clarified by ultracentrifugation at 400,000 *g* for 45 min. The resulting supernatant was the cytosol fraction, and the pellet was the membrane fraction. Both were mixed with SDS-PAGE sample buffer to the same final volume, and the proteins were analyzed by Western blotting.

Recombinant proteins

All recombinant proteins were expressed in Sf9 cells with the Bac-to-Bac Baculovirus Expression System (Invitrogen). WAVE2 and Abi1 were tagged with GST at their COOH termini and expressed with pFastBac. PIR121 was tagged with GST at its COOH terminus and was coexpressed with Nap1 in the pFastBac Dual vector. WAVE2 tagged with GST and Abi1 were also coexpressed in the pFastBac Dual vector for better expression. Approximately half of WAVE2 that coexpressed with Abi1 was complexed with Abi1 after purification. Proteins were purified as described previously (Miki et al., 2000).

Determination of Kd value using a dual polarization interferometer

The interaction of WAVE2 with the coiled-coil region of Abi1 or the SH3 domain of IRSp53 using a dual polarization interferometer was investigated with AnaLight Bio 200 (Farfield) as described previously (Oikawa et al., 2004). WAVE2 was cross-linked on sensortip coated with amine with BS3 cross-linker (Sigma-Aldrich). The Kd values were calculated from curve fitting.

Actin polymerization assay

Actin polymerization assays were performed in XB buffer as described previously (Miki et al., 2000). The Arp2/3 complex was used at a concentration of 50 nM.

Liposome cosedimentation assay and actin polymerization assay on PIP_3-coated beads

PIP_3, PC, and PI as well as PIP_3-coated beads were obtained from Echelon Biosciences. Liposome cosedimentation assays were performed as described previously (Oikawa et al., 2004). For actin filament formation assays on PIP_3 beads, 40 μg/ml WAVE2-GST coexpressed with Abi1, 100 μg/ml GST-IRSp53, and 30 μg/ml GTPγS- or GDP-loaded GST-Rac in 10 μl XB buffer were incubated with 2 μl PIP_3-coated beads. WAVE2 complex from A431 cells (0.5 μg/ml WAVE2) was also incubated with PIP_3-coated beads and Rac. After incubation at room temperature for 20 min, beads were washed with 100 μl XB buffer. Beads were then mixed with 50 μl XB buffer containing 50 nM Arp2/3 complex, 2 μM G-actin, 2 mg/ml BSA, and 2 unit/ml rhodamine-labeled phalloidin (Invitrogen) on ice. After incubation for 20 min on ice, 10 μl of bead-containing solution was placed between 18 × 18-mm BSA-coated glass and slide glass. After 10 min at room temperature, actin filaments were observed by phalloidin fluorescence. Fluorescence intensity was calculated by ImageJ software with the Oval profile plug-in (National Institutes of Health).

Image acquisition and processing

All fluorescent images were taken through a microscope (Eclipse E600; Nikon) with a confocal microscopy system (Radiance 2000; Bio-Rad Laboratories) at room temperature. Fluorochromes used include AlexaFluor488, 546, and 647 and rhodamine (all purchased from Invitrogen). A 60× NA 1.40 oil immersion objective (Nikon) was used. Images were assembled with Adobe Photoshop. In each plate, photographs were cropped, and each fluorochrome was adjusted identically for brightness and contrast to represent the observed images. Time-lapse images were taken through a phase-contrast microscope (Axiovert S100; Carl Zeiss MicroImaging, Inc.) with a camera (CCD-782-Y/HS; Princeton Instruments). A 40× NA 1.30 FLUAR oil immersion objective (Carl Zeiss MicroImaging, Inc.) was used.

Western blotting and densitometry

The samples were electrophoresed in SDS-PAGE gels, transferred to polyvinylidene difluoride membrane, blocked with 5% nonfat dry milk in PBS and 0.1% Tween 20, incubated with primary antibodies, and incubated with alkaline-phosphatase–conjugated goat IgG secondary antibodies (Promega) followed by incubation with NBT/BCIP substrate (Roche). Resulting blots were scanned with a calibrated densitometer (GS-710; Bio-Rad Laboratories) and quantified with ImageJ software.

Online supplemental material

Fig. S1 shows the WAVE2 complex and IRSp53 in A431 cells. Fig S2 shows the involvement of IRSp53 in ruffle formation in MEFs. Fig. S3 shows silver-stained gel images of fractionated WAVE2 in Fig. 5 (F–K). Fig. S4 shows the reconstituted recombinant proteins used in this study. Fig. S5 shows the actin polymerization on PIP_3-coated beads by the WAVE2 complex or WAVE2 in the presence of IRSp53 and Rac. Videos 1 and 2 show cells treated with RNAi under stimulation. Online supplemental material is available at http://www.jcb.org/cgi/content/full/jcb.200509067/DC1.

We thank Dr. Tadashi Yamamoto, Dr. Tohru Tezuka, Ms. Kazuko Nakahira, and other members of our laboratories (Institute of Medical Science, University of Tokyo, Tokyo, Japan) for antibodies, technical support, and helpful discussions.

This work was supported by grants-in-aid from the Ministry of Education, Culture, Sports, Science and Technology of Japan and from the Japan Science and Technology Corporation.

Submitted: 12 September 2005
Accepted: 13 April 2006

References

Bershadsky, A. 2004. Magic touch: how does cell-cell adhesion trigger actin assembly? *Trends Cell Biol.* 14:589–593.

Choi, J., J. Ko, B. Racz, A. Burette, J.R. Lee, S. Kim, M. Na, H.W. Lee, K. Kim, R.J. Weinberg, and E. Kim. 2005. Regulation of dendritic spine morphogenesis by insulin receptor substrate 53, a downstream effector of Rac1 and Cdc42 small GTPases. *J. Neurosci.* 25:869–879.

Chung, C.Y., S. Funamoto, and R.A. Firtel. 2001. Signaling pathways controlling cell polarity and chemotaxis. *Trends Biochem. Sci.* 26:557–566.

Connolly, B.A., J. Rice, L.A. Feig, and R.J. Buchsbaum. 2005. Tiam1-IRSp53 complex formation directs specificity of rac-mediated actin cytoskeleton regulation. *Mol. Cell. Biol.* 25:4602–4614.

Cossart, P., and P.J. Sansonetti. 2004. Bacterial invasion: the paradigms of enteroinvasive pathogens. *Science.* 304:242–248.

Echarri, A., M.J. Lai, M.R. Robinson, and A.M. Pendergast. 2004. Abl interactor 1 (Abi-1) wave-binding and SNARE domains regulate its nucleocytoplasmic shuttling, lamellipodium localization, and wave-1 levels. *Mol. Cell. Biol.* 24:4979–4993.

Eden, S., R. Rohatgi, A.V. Podtelejnikov, M. Mann, and M.W. Kirschner. 2002. Mechanism of regulation of WAVE1-induced actin nucleation by Rac1 and Nck. *Nature.* 418:790–793.

Gautreau, A., H.Y. Ho, J. Li, H. Steen, S.P. Gygi, and M.W. Kirschner. 2004. Purification and architecture of the ubiquitous Wave complex. *Proc. Natl. Acad. Sci. USA.* 101:4379–4383.

Govind, S., R. Kozma, C. Monfries, L. Lim, and S. Ahmed. 2001. Cdc42Hs facilitates cytoskeletal reorganization and neurite outgrowth by localizing the 58-kD insulin receptor substrate to filamentous actin. *J. Cell Biol.* 152:579–594.

Hall, A. 1998. Rho GTPase and the actin cytoskeleton. *Science.* 279:509–514.

Innocenti, M., A. Zucconi, A. Disanza, E. Frittoli, L.B. Areces, A. Steffen, T.E. Stradal, P.P. Di Fiore, M.F. Carlier, and G. Scita. 2004. Abi1 is essential for the formation and activation of a WAVE2 signalling complex. *Nat. Cell Biol.* 6:319–327.

Krugmann, S., I. Jordens, K. Gevaert, M. Driessens, J. Vandekerckhove, and A. Hall. 2001. Cdc42 induces filopodia by promoting the formation of an IRSp53:Mena complex. *Curr. Biol.* 11:1645–1655.

Kunda, P., G. Craig, V. Dominguez, and B. Baum. 2003. Abi, Sra1, and Kette control the stability and localization of SCAR/WAVE to regulate the formation of actin-based protrusions. *Curr. Biol.* 13:1867–1875.

Kurisu, S., S. Suetsugu, D. Yamazaki, H. Yamaguchi, and T. Takenawa. 2005. Rac-WAVE2 signaling is involved in the invasive and metastatic phenotypes of murine melanoma cells. *Oncogene*. 24:1309–1319.

Leng, Y., J. Zhang, K. Badour, E. Arpaia, S. Freeman, P. Cheung, M. Siu, and K. Siminovitch. 2005. Abelson-interactor-1 promotes WAVE2 membrane translocation and Abelson-mediated tyrosine phosphorylation required for WAVE2 activation. *Proc. Natl. Acad. Sci. USA.* 102:1098–1103.

Miki, H., M. Fukuda, E. Nishida, and T. Takenawa. 1999. Phosphorylation of WAVE downstream of mitogen-activated protein kinase signaling. *J. Biol. Chem.* 274:27605–27609.

Miki, H., H. Yamaguchi, S. Suetsugu, and T. Takenawa. 2000. IRSp53 is an essential intermediate between Rac and WAVE in the regulation of membrane ruffling. *Nature.* 408:732–735.

Millard, T.H., G. Bompard, M.Y. Heung, T.R. Dafforn, D.J. Scott, L.M. Machesky, and K. Futterer. 2005. Structural basis of filopodia formation induced by the IRSp53/MIM homology domain of human IRSp53. *EMBO J.* 24:240–250.

Nagai, T., K. Ibata, E.S. Park, M. Kubota, K. Mikoshiba, and A. Miyawaki. 2002. A variant of yellow fluorescent protein with fast and efficient maturation for cell-biological applications. *Nat. Biotechnol.* 20:87–90.

Oikawa, T., H. Yamaguchi, T. Itoh, M. Kato, T. Ijuin, D. Yamazaki, S. Suetsugu, and T. Takenawa. 2004. PtdIns(3,4,5)P3 binding is necessary for WAVE2-induced formation of lamellipodia. *Nat. Cell Biol.* 6:420–426.

Rickert, P., O.D. Weiner, F. Wang, H.R. Bourne, and G. Servant. 2000. Leukocytes navigate by compass: roles of PI3Kgamma and its lipid products. *Trends Cell Biol.* 10:466–473.

Ridley, A.J., M.A. Schwartz, K. Burridge, R.A. Firtel, M.H. Ginsberg, G. Borisy, J.T. Parsons, and A.R. Horwitz. 2003. Cell migration: integrating signals from front to back. *Science.* 302:1704–1709.

Rogers, S.L., U. Wiedemann, N. Stuurman, and R.D. Vale. 2003. Molecular requirements for actin-based lamella formation in *Drosophila* S2 cells. *J. Cell Biol.* 162:1079–1088.

Shi, J., G. Scita, and J.E. Casanova. 2005. WAVE2 signaling mediates invasion of polarized epithelial cells by *Salmonella typhimurium*. *J. Biol. Chem.* 280:29849–29855.

Sini, P., A. Cannas, A.J. Koleske, P.P. Di Fiore, and G. Scita. 2004. Abl-dependent tyrosine phosphorylation of Sos-1 mediates growth-factor-induced Rac activation. *Nat. Cell Biol.* 6:268–274.

Snapper, S.B., F. Takeshima, I. Anton, C.H. Liu, S.M. Thomas, D. Nguyen, D. Dudley, H. Fraser, D. Purich, M. Lopez-Ilasaca, et al. 2001. N-WASP deficiency reveals distinct pathways for cell surface projections and microbial actin-based motility. *Nat. Cell Biol.* 3:897–904.

Steffen, A., K. Rottner, J. Ehinger, M. Innocenti, G. Scita, J. Wehland, and T.E. Stradal. 2004. Sra-1 and Nap1 link Rac to actin assembly driving lamellipodia formation. *EMBO J*. 23:749–759.

Suetsugu, S., and T. Takenawa. 2003. Regulation of cortical actin networks in cell migration. *Int. Rev. Cytol.* 229:245–286.

Suetsugu, S., H. Miki, and T. Takenawa. 1999. Identification of two human WAVE/SCAR homologues as general actin regulatory molecules which associate with Arp2/3 complex. *Biochem. Biophys. Res. Commun.* 260:296–302.

Suetsugu, S., D. Yamazaki, S. Kurisu, and T. Takenawa. 2003. Differential roles of WAVE1 and WAVE2 in dorsal and peripheral ruffle formation for fibroblast cell migration. *Dev. Cell.* 5:595–609.

Takenawa, T., and H. Miki. 2001. WASP and WAVE family proteins: key molecules for rapid rearrangement of cortical actin filaments and cell movement. *J. Cell Sci.* 114:1801–1809.

Yamazaki, D., S. Suetsugu, H. Miki, Y. Kataoka, S. Nishikawa, T. Fujiwara, N. Yoshida, and T. Takenawa. 2003. WAVE2 is required for directed cell migration and cardiovascular development. *Nature.* 424:452–456.

Yamazaki, D., T. Fujiwara, S. Suetsugu, and T. Takenawa. 2005. A novel function of WAVE in lamellipodia: WAVE1 is required for stabilization of lamellipodial protrusions during cell spreading. *Genes Cells.* 10:381–392.

Yan, C., N. Martinez-Quiles, S. Eden, T. Shibata, F. Takeshima, R. Shinkura, Y. Fujiwara, R. Bronson, S.B. Snapper, M.W. Kirschner, et al. 2003. WAVE2 deficiency reveals distinct roles in embryogenesis and Rac-mediated actin-based motility. *EMBO J.* 22:3602–3612.